An All D-Amino Acid Opioid Peptide with Central Analgesic Activity from a Combinatorial Library

C. T. Dooley, N. N. Chung, B. C. Wilkes, P. W. Schiller, J. M. Bidlack, G. W. Pasternak, R. A. Houghten*

A synthetic combinatorial library containing 52,128,400 D-amino acid hexapeptides was used to identify a ligand for the μ opioid receptor. The peptide, Ac-rfwink-NH_2, bears no resemblance to any known opioid peptide. Simulations using molecular dynamics, however, showed that three amino acid moieties have the same spatial orientation as the corresponding pharmacophoric groups of the opioid peptide PLO17. Ac-rfwink-NH_2 was shown to be a potent agonist at the μ receptor and induced long-lasting analgesia in mice. Analgesia produced by intraperitoneally administered Ac-rfwink-NH_2 was blocked by intracerebroventricular administration of naloxone, demonstrating that this peptide may cross the blood-brain barrier.

Synthetic combinatorial libraries (SCLs) (*1*, *2*), composed of tens of millions of soluble peptides, have been shown to be highly effective in the rapid identification of opioid peptides such as methionine- and leucine-enkephalin (*3*, *4*). Also, an N-acetylated library made up of 52 million hexapeptides was used to identify the acetalins (*5*), potent opioid antagonists bearing no sequence homology to any of the known opioid peptides. A similar library of N-acetylated hexapeptides, composed entirely of D-amino acids (*6*) and represented as Ac-$o_1o_2$xxxx-NH_2 (Ac, CH_3CO) (Fig. 1), has now been used to identify an "all D" opioid peptide. The library (*7*) was screened for its ability to inhibit the binding of [^{3}H][D-Ala^2,MePhe^4,Gly^5-ol]enkephalin (DAMGO) to rat brain homogenates (Fig. 1). An iterative selection process (*8*) was carried out on the most active mixtures (*9*) in order to define each of the four mixture positions (x) (Ac-$o_1o_2$xxxx-NH_2→Ac-$o_1o_2o_3o_4o_5o_6$-NH_2). At each iteration (Table 1), the number of peptides within each mixture was reduced by a factor of 19. Ac-rfwink-NH_2 [50% inhibition concentration (IC_{50}) = 18 nM] (*10*) was the most active individual peptide found (*11*).

Ac-rfwink-NH_2 exhibited high selectivity for μ receptors [inhibition constant (K_i) values: μ_1 = 16 ± 0.5 nM, μ_2 = 41 ± 4.8 nM] (*12*). Ac-rfwink-NH_2 inhibited the binding of the δ-selective peptide [^{3}H][D-Pen^2, D-Pen^5]enkephalin (DPDPE) only poorly (K_i > 1500 nM). Furthermore, Ac-rfwink-NH_2 had very low affinity at both the κ_1 (K_i > 2000 nM) and κ_2 (K_i > 5000 nM) receptor subtypes and only modest affinity for κ_3 receptors (K_i = 288 ± 71 nM).

Ac-rfwink-NH_2 was shown to be a full agonist in the guinea pig ileum assay (IC_{50} = 433 ± 43 nM), exhibiting activity 50% lower than that observed for leu-enkephalin (IC_{50} = 246 ± 39 nM) and one-twentieth that of PLO17 (IC_{50} = 21 ± 2 nM). This activity was antagonized by naloxone at a low concentration (dissociation constant, K_e = 3.80 nM), indicating that it was an opioid effect mediated through interaction with μ opioid receptors (*13*). Ac-rfwink-NH_2 was also tested for its ability to inhibit electrically evoked contractions of the mouse vas deferens, a tissue containing predominantly δ receptors. In this assay system, the peptide was 100 times less potent than leu-enkephalin. The agonist activity of this "all D" peptide is noteworthy because an antagonist only has to bind to a receptor in order to block another ligand from binding, whereas an agonist must not only bind, but must also induce a conformational change in the receptor in order to achieve signal transduction.

Like most linear peptides, Ac-rfwink-NH_2 has substantial structural flexibility and is able to assume a large number of low-energy conformers. Because the amino terminal is acetylated, the positively charged guanidinium group of the Arg^1 side chain may play the role of the NH_2-termi-

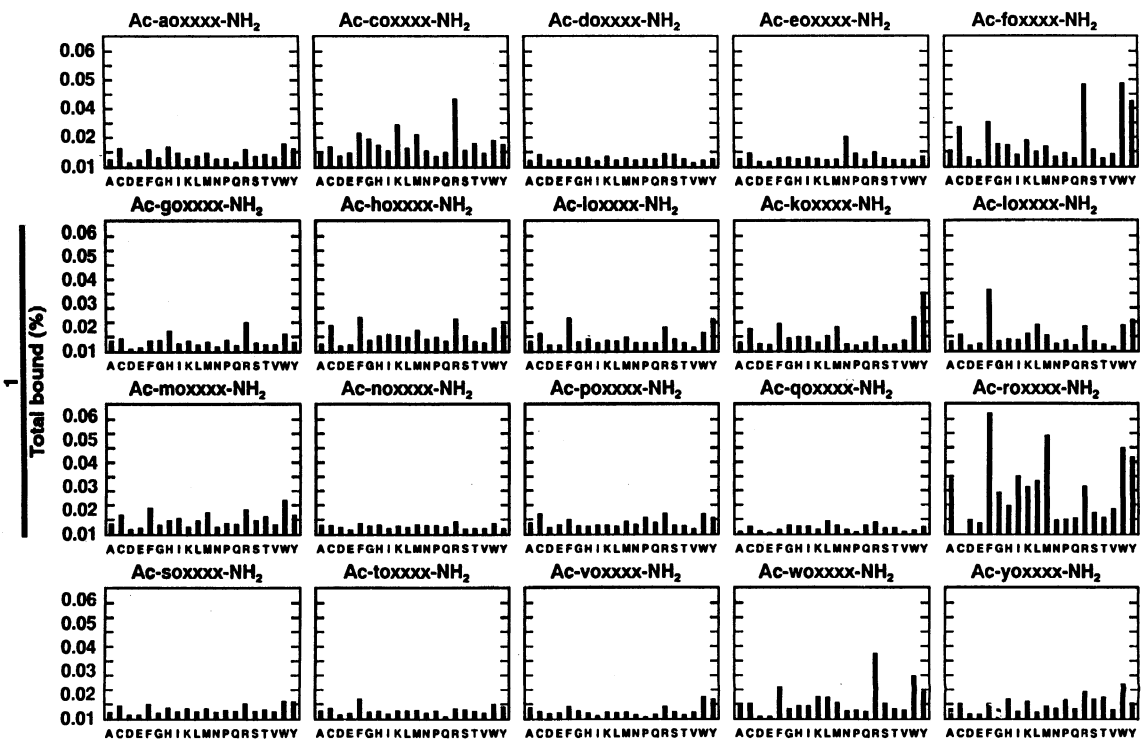

Fig. 1. Initial screening of the SCL (Ac-ooxxxx-NH_2, lowercase lettering represents D-enantiomers) for ability to inhibit the binding of 7 nM[3] H-DAMGO to crude rat brain homogenates. The first two positions (o_1 and o_2) are individually defined (o) with each of the 20 D-amino acids (*6*). The remaining four positions consist of mixtures (x) of 19 D-amino acids (cysteine excluded, glycine included). The library consists of 400 mixtures; each mixture contains 130,321 (19^4) peptides; the SCL in total is made up of 52,128,400 different peptides. The individual graphs are separated first by amino acid (o_1), with the individual bars in each graph representing the individual amino acids making up the second position (o_2). IC_{50} values were subsequently determined for all mixtures exhibiting over 70% inhibition (see Table 1).

Table 1. Inhibition of [^{3}H]DAMGO binding by peptide mixtures derived from the acetylated SPCL. The IC_{50} values of the inhibitory peptide mixtures obtained at each iterative step are illustrated for (a) peptide mixtures from Ac-roxxxx-NH_2 of the SCL, and (b to e) mixtures defining the third, fourth, fifth, and sixth positions (*8*). The IC_{50} value of the peptide mixture found to be most effective in the previous mixture is boxed for comparison. Iterations carried out for Ac-ryxxxx-NH_2 (*9*) ultimately yielded peptides of lower activity than those of Ac-rfxxxx-NH_2; iterations of the latter are shown below. The IC_{50} values for Ac-crxxxx-NH_2, Ac-frxxxx-NH_2, Ac-fwxxxx-NH_2, Ac-fyxxxx-NH_2, Ac-kyxxxx-NH_2, and Ac-lfxxxx-NH_2 were all greater than 40,000 nM. The IC_{50} value for Ac-wrxxxx-NH_2 was 24,000 nM.

a		b		c		d		e	
Ac-roxxxx-NH_2	IC_{50} ± SE (nM)	Ac-rfoxxx-NH_2	IC_{50} ± SE (nM)	Ac-rfwoxx-NH_2	IC_{50} ± SE (nM)	Ac-rfwiox-NH_2	IC_{50} ± SE (nM)	Ac-rfwino-NH_2	IC_{50} ± SE (nM)
Ac-ryxxxx-NH_2	7300 ±600	Ac-rfwxxx-NH_2	900 ±300	Ac-rfwwxx-NH_2	400 ±15	Ac-rfwinx-NH_2	200 ±1	Ac-rfwink-NH_2	18 ±4
Ac-rwxxxx-NH_2	10000 ±700	Ac-rffxxx-NH_2	2000 ±500	Ac-rfwixx-NH_2	500 ±200	Ac-rfwiax-NH_2	350 ±90	Ac-rfwinr-NH_2	27 ±13
Ac-rfxxxx-NH_2	12000 ±2000	Ac-rfhxxx-NH_2	2400 ±100	Ac-rfwlxx-NH_2	1000 ±300	Ac-rfwikx-NH_2	370 ±90	Ac-rfwina-NH_2	37 ±13
Ac-rmxxxx-NH_2	16000 ±200	Ac-rfyxxx-NH_2	2500 ±200	Ac-rfwmxx-NH_2	1000 ±300	Ac-rfwirx-NH_2	460 ±130	Ac-rfwinx-NH_2	110 ±42
Ac-rlxxxx-NH_2	24000 ±2900	Ac-rfixxx-NH_2	5500 ±400	Ac-rfwfxx-NH_2	1000 ±400	Ac-rfwixx-NH_2	480 ±150	Ac-rfwins-NH_2	130 ±55
Ac-rsxxxx-NH_2	37000 ±8000	Ac-rfvxxx-NH_2	6900 ±100	Ac-rfwxxx-NH_2	1500 ±200	Ac-rfwisx-NH_2	490 ±140	Ac-rfwinp-NH_2	130 ±31
Ac-rgxxxx-NH_2	48000 ±3900	Ac-rfcxxx-NH_2	9800 ±2900	Ac-rfwyxx-NH_2	1500 ±200	Ac-rfwimx-NH_2	500 ±140	Ac-rfwinn-NH_2	130 ±67
Ac-raxxxx-NH_2	48000 ±3800	Ac-rfmxxx-NH_2	12000 ±700	Ac-rfwcxx-NH_2	1600 ±700	Ac-rfwifx-NH_2	690 ±240	Ac-rfwinq-NH_2	140 ±42
Ac-rtxxxx-NH_2	54000 ±7900	Ac-rfaxxx-NH_2	12000 ±2600	Ac-rfwnxx-NH_2	2000 ±200	Ac-rfwilx-NH_2	700 ±210	Ac-rfwing-NH_2	170 ±78
Ac-rixxxx-NH_2	57000 ±5100	Ac-rflxxx-NH_2	13000 ±700	Ac-rfwsxx-NH_2	2300 ±800	Ac-rfwitx-NH_2	780 ±140	Ac-rfwinm-NH_2	180 ±69
Ac-rnxxxx-NH_2	57000 ± ND	Ac-rfkxxx-NH_2	14000 ±5500	Ac-rfwgxx-NH_2	2400 ±900	Ac-rfwigx-NH_2	1100 ±44	Ac-rfwinh-NH_2	200 ±170
Ac-rcxxxx-NH_2	57000 ±200	Ac-rfsxxx-NH_2	14000 ±3800	Ac-rfwhxx-NH_2	2400 ±1200	Ac-rfwiwx-NH_2	1200 ±340	Ac-rfwint-NH_2	230 ±91
Ac-rhxxxx-NH_2	78000 ±16000	Ac-rfrxxx-NH_2	15000 ±5000	Ac-rfwpxx-NH_2	2700 ±900	Ac-rfwihx-NH_2	1300 ±320	Ac-rfwiny-NH_2	460 ±650
Ac-rpxxxx-NH_2	110000 ±7800	Ac-rftxxx-NH_2	21000 ±5700	Ac-rfwaxx-NH_2	2800 ±1100	Ac-rfwivx-NH_2	1500 ±280	Ac-rfwinl-NH_2	680 ±390
Ac-rvxxxx-NH_2	110000 ±4600	Ac-rfnxxx-NH_2	21000 ±1000	Ac-rfwvxx-NH_2	3700 ±1400	Ac-rfwiyx-NH_2	1500 ±280	Ac-rfwinc-NH_2	720 ±280
Ac-rqxxxx-NH_2	120000 ±17000	Ac-rfqxxx-NH_2	23000 ±1100	Ac-rfwtxx-NH_2	3800 ±800	Ac-rfwiqx-NH_2	2300 ±450	Ac-rfwinf-NH_2	770 ±510
Ac-rkxxxx-NH_2	150000 ±29000	Ac-rfkxxx-NH_2	23000 ±4100	Ac-rfwqxx-NH_2	4200 ±1600	Ac-rfwicx-NH_2	2400 ±570	Ac-rfwinw-NH_2	790 ±130
Ac-rnxxxx-NH_2	160000 ±37000	Ac-rfdxxx-NH_2	50000 ±100	Ac-rfwkxx-NH_2	4400 ±2100	Ac-rfwiix-NH_2	2800 ±150	Ac-rfwine-NH_2	960 ±650
Ac-rdxxxx-NH_2	210000 ±71000	Ac-rfexxx-NH_2	68000 ±7200	Ac-rfwnxx-NH_2	4500 ±2000	Ac-rfwipx-NH_2	3700 ±700	Ac-rfwind-NH_2	1100 ±280
Ac-rexxxx-NH_2	320000 ±200	Ac-rfpxxx-NH_2	69000 ±7000	Ac-rfwexx-NH_2	15000 ±6400	Ac-rfwidx-NH_2	8000 ±2000	Ac-rfwinv-NH_2	1300 ±770
		Ac-rfgxxx-NH_2	ND	Ac-rfwdxx-NH_2	33000 ±7800	Ac-rfwiex-NH_2	11000 ±2300	Ac-rfwini-NH_2	5600 ±3500

nal amino group always present in "classical" opioid peptides, resulting in an electrostatic interaction with a negatively charged receptor moiety. Furthermore, the Phe^2 and Trp^3 aromatic residues in Ac-rfwink-NH_2 may correspond to the Tyr^1 residue and the Phe^3 (or the Phe^4) residue, respectively, in opioid peptides such as morphiceptin or the enkephalins. Molecular dynamics simulations generated a number of low-energy conformers of Ac-rfwink-NH_2, one of which showed good spatial overlap of the three defined pharmacophoric moieties with the corresponding pharmacophoric groups of PLO17 (Fig. 2). PLO17 (H-YPF(NMe)*p*-NH_2), an analog of morphiceptin, is a potent and selective μ agonist. A model of its bioactive conformation has recently been proposed (*14*) . These results provide a possible explanation for the fact that these two peptides, which have entirely different primary structures, bind to and activate the same receptor. It should be noted that Ac-rfwink-NH_2 lacks the hydroxyl group common to many opioid peptides. It has been previously demonstrated (*15*) that omission of the tyrosine hydroxyl group in these opioids, in many instances, still results in compounds retaining substantial agonist potency if the resulting loss in receptor interaction energy can be compensated for by favorable interactions of other structural elements of the ligand with the receptor. In the case of Ac-rfwink-NH_2, residues in the carboxyl-terminal portion of the peptide may interact with the receptor and compensate for its lack of a hydroxyl group.

In the mouse 55°C warm-water tail-flick test, an intracerebroventricular (i.c.v.) injection of Ac-rfwink-NH_2 produced antinociception in a dose-dependent manner (Fig. 3A). Ac-rfwink-NH_2 (3 nmol), given 20 min before testing, produced 100% antinociception; this maximal antinociception lasted for 120 min. The duration of the analgesic effect of Ac-rfwink-NH_2 is noteworthy. Ac-rfwink-NH_2 (1 nmol or greater) produced 25% or greater antinociception for at least 300 min after a single injection (Fig. 3A). Morphine (10 nmol) produced 100% antinociception, but 25% or greater antinociception was observed for only 140 min, and a 1-nmol dose of morphine produced 25% or greater analgesia for only 80 min (Fig. 3B). Both the duration of action (Fig. 3) and the potency

C. T. Dooley, Torrey Pines Institute for Molecular Studies, San Diego, CA 92121, USA.
N. N. Chung, B.C. Wilkes, P. W. Schiller, Laboratory of Chemical Biology and Peptide Research, Clinical Research Institute of Montreal, Montreal H2W 1R7, Canada.
J. M. Bidlack, Department of Pharmacology, University of Rochester Medical Center, Rochester, New York 14642, USA.
G. W. Pasternak, Department of Neurology, Memorial Sloan-Kettering Cancer Center, Harvard Building 808, New York, NY 10021, USA.
R. A. Houghten, Torrey Pines Institute for Molecular Studies and Houghten Pharmaceuticals Inc., San Diego, CA 92121, USA.
*To whom correspondence should be addressed.

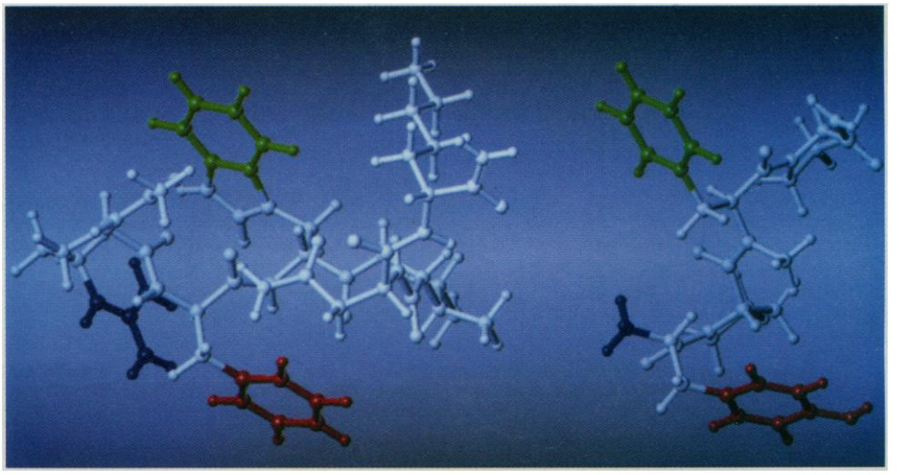

Fig. 2. Comparison of a low-energy conformer of Ac-rfwink-NH_2 (**left**) with the proposed bioactive conformation of the morphiceptin analog PLO17 (14) (**right**). Conformations of Ac-rfwink-NH_2 were generated by molecular dynamics simulation and were subjected to simulated annealing with distance constraints between the aromatic rings and the guanidinium group, on the basis of distances between the corresponding functional groups in the PLO17 model. There is good spatial overlap between the three proposed pharmacophoric groups in the two structures (root-mean-square deviation of 0.85Å).

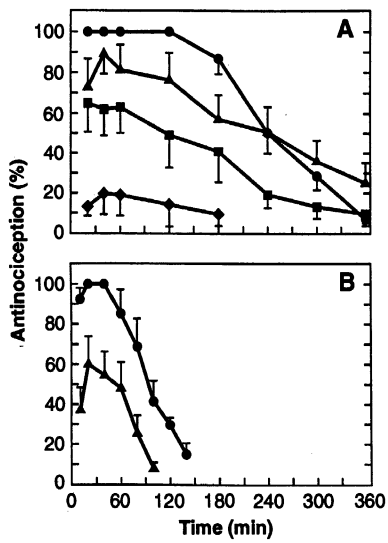

Fig. 3. Time-course lines for varying i.c.v. doses of Ac-rfwink-NH_2 (**A**) or morphine (**B**) in the mouse 55°C warm-water tail-flick test (*16*). At 20 min after i.c.v. injection, an ED_{50} value of 0.6 (0.22 to 1.6) nmol and 1.29 (0.83 to 2.0) nmol were obtained for Ac-rfwink-NH_2 and morphine (*16*), respectively. Ac-rfwink-NH_2 (1 nmol or greater) produced 25% or greater antinociception for at least 300 min after a single i.c.v. injection. Morphine (10 and 1 nmol) produced 25% or greater antinociception for 140 and 80 min, respectively. Ac-rfwink-NH_2: (●) 3 nmol, (▲) 1 nmol, (■) 0.6 nmol, and (◆) 0.3 nmol; morphine: (●) 10 nmol, and (▲) 1 nmol.

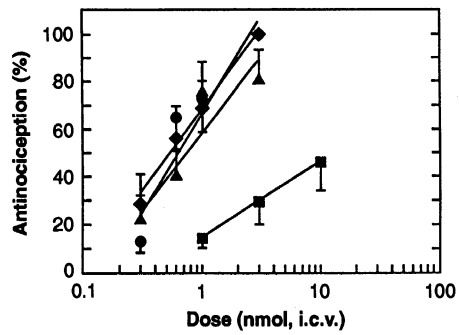

Fig. 4. Dose-response lines for i.c.v. Ac-rfwink-NH_2 in the absence or presence of either the μ-selective irreversible antagonist β-FNA, the δ-selective antagonist ICI 174,864 or the κ-selective antagonist nor-BNI in the mouse 55°C warm-water tail-flick test (*16*). Mice were pretreated with either a single i.c.v. injection of β-FNA (20 nmol, −24 hours before testing), or with ICI 174,864 (4 nmol) or nor-BNI (1 nmol), administered simultaneously with Ac-rfwink-NH_2, 20 min before testing. Neither nor-BNI [ED_{50} = 0.66 (0.36 to 1.1) nmol] nor ICI 174,864 [ED_{50} = 0.55 (0.41 to 0.73) nmol] altered the dose-response curve for Ac-rfwink-NH_2. The μ-selective antagonist β-FNA shifted the dose-response line for Ac-rfwink-NH_2 to the right, indicating that Ac-rfwink-NH_2 produced antinociception through μ opioid receptors. (●) Ac-rfwink-NH_2, (◆) + ICI 174,864 4 nmol, (▲) + nor-BNI 1 nmol, and (■) + β-FNA 20 nmol −24 hours.

of Ac-rfwink-NH_2 [median effective dose (ED_{50}) = 0.6 nmol, 95% confidence limits: 0.22 to 1.6 nmol] were approximately twofold greater than the values obtained with morphine (ED_{50} = 1.29 nmol, 95% confidence limits: 0.83 to 2.0 nmol) (*16*). As shown in Fig. 4, a single i.c.v. injection of the μ-selective irreversible antagonist β-funaltrexamine (β-FNA), given 24 hours before testing, shifted the dose-response line for Ac-rfwink-NH_2 to the right. In contrast, the δ-selective antagonist ICI 174,864 and the κ-selective antagonist nor-binaltorphimine (nor-BNI) had no effect on the antinociception induced by Ac-rfwink-NH_2, indicating that Ac-rfwink-NH_2 produced antinociception through the μ opioid receptor. In addition, intraperitoneal (i.p.) administration of either Ac-rfwink-NH_2 (10 mg/kg) or morphine (10 mg/kg) 30 min before testing resulted in 51 ± 11% and 47 ± 9% antinociception, respectively. An i.c.v. injection of the opioid antagonist naloxone (3 nmol), given 15 min after the i.p. administration of either Ac-rfwink-NH_2 or morphine, reduced antinociception to 13 ± 4% and 2 ± 2%, respectively ($P \leq 0.05$ in comparison to mice treated only with the corresponding agonist). These results strongly suggest that after i.p. injection, Ac-rfwink-NH_2, like morphine, produces antinociception through supraspinal μ opioid receptors. The fact that an i.p. injection of Ac-rfwink-NH_2 produced antinociception mediated by supraspinal μ opioid receptors is of interest, because this peptide must migrate from the i.p. space into the bloodstream and then into brain capillaries. Unlike peptides comprised of naturally occurring L-amino acids, a D-amino acid peptide will not be degraded by proteases. Therefore, peripherally administered Ac-rfwink-NH_2 can be expected to remain intact, which will increase both the amount of peptide crossing the blood-brain barrier and the resulting analgesia. Although the potency of Ac-rfwink-NH_2 in the guinea pig ileum assay was much lower than that of PLO17, the ability of Ac-rfwink-NH_2 to cross the blood-brain barrier and its long duration of action makes this peptide of interest for in vivo studies. The identification of this unique peptide and its activity at the μ receptor advances our understanding of the binding interactions involved and serves to further confirm the power of the combinatorial library approach for the discovery of new, biologically active compounds.

REFERENCES AND NOTES

1. R. A. Houghten *et al.*, *Nature* **354**, 84 (1991).
2. R. A. Houghten *et al.*, *BioTechniques* **13**, 412 (1992).
3. R. A. Houghten and C. T. Dooley, *BioMed. Chem. Lett.* **3**, 405 (1993).
4. C. T. Dooley and R. A. Houghten, *Life Sci.* **52**, 1509 (1993).
5. C. T. Dooley, N. N. Chung, P. W. Schiller, R. A. Houghten, *Proc. Natl. Acad. Sci. U.S.A.* **90**, 10811 (1993).
6. Glycine has no D enantiomer, but for simplicity is considered here as a D-amino acid.
7. The library was synthesized as described previously with only D-amino acids; xxxx-resin was prepared by a process of dividing, coupling, and recombining the individual resins (*1, 2*). Two individual amino acids, o_1 and o_2, were added by simultaneous multiple peptide synthesis (*17*). After acetylation, deprotection, and cleavage from the resins, each of the 400 peptide mixtures was extracted with water to yield a final peptide concentration of 1 to 3 mg/ml. Preparation of rat brain membranes and the receptor binding assay were done as described in (*4*). Each tube in the screening assay contained 0.08 mg of peptide mixture per milliliter, 0.5 ml of membrane suspension (0.1 mg of protein), 7 nM ^{3}H-labeled DAMGO [specific activity 36 Ci/mmol, obtained from the National Institute on Drug Abuse (NIDA) repository through Chiron Mimotopes Peptide Systems (San Diego, CA)], and 50 μl of peptide mixture in 50 mM tris-HCl buffer (pH 7.4). The final volume was 0.65 ml.
8. For each iteration, 20 new mixtures are synthesized such that one of the x positions is individually defined with one of the 20 D-amino acids (o). Thus, the definition of the third position, Ac-rfoxxx-NH_2, is represented as Ac-rfaxxx-NH_2, Ac-rfcxxx-NH_2. . . through Ac-rfyxxx-NH_2.
9. For those cases in which the most active mixture is not described in the next iteration, the iterations for these mixtures were completed. However, the individual peptides obtained were not as active as those described here.
10. Single-letter code; lowercase letters indicate D-amino acids: a, Ala; c, Cys; d, Asp; e, Glu; f, Phe; g, Gly; h, His; i, Ile; k, Lys; l, Leu; m, Met; n, Asn; p, Pro; q, Gln; r, Arg; s, Ser; t, Thr; v, Val; w, Trp; and y, Tyr.
11. Additions to the amino-terminus of Ac-rfwink-NH_2 (that is, Ac-orfwink-NH_2) resulted in substantial decreases in binding (sixfold or greater). Also, additions to the carboxyl-terminus (Ac-rfwinko-NH_2) in every case resulted in a twofold or greater decrease in activity. Omission of the N-acetyl group, rfwink-NH_2, produced a 200-fold decrease in activity (IC_{50} = 3300 nM) when compared to the acetylated form. The corresponding peptide, with a carboxylate group (Ac-rfwink-OH), was found to be six times less active than the parent peptide amide. Individual replacement of each of the D-amino acids with their L-enantiomer counterparts resulted in decreases in activity ranging from 2- to 200-fold, with the most active being the L-Lys^6 analog, which had an IC_{50} of 36 nM (half as active as Ac-rfwink-NH_2). Ac-rfwink-NH_2: U.S. Patent No. 5,367,053.
12. Binding assays for the opioid receptor subtypes were carried out as described previously for μ_1 and μ_2 (*18*), δ (*19*), κ_1, κ_2, and κ_3 (*20, 21*). The guinea pig ileum (*22*) and mouse vas deferens (*23*) bioassays were carried out as reported elsewhere (*24, 25*). Logarithmic dose-response curves were obtained for each compound, and IC_{50} values were determined. The K_e value for naloxone as antagonist was determined from the ratio of IC_{50} values obtained with Ac-rfwink-NH_2 in the presence and absence of a fixed naloxone concentration (5 nM) (*26*).
13. C. Chavkin, I. F. James, A. Goldstein, *Science* **215**, 413 (1982).
14. T. Yamazaki, S. Ro, M. Goodman, N. N. Chung, P. W. Schiller, *J. Med Chem.* **36** 708 (1993).
15. P. W. Schiller and J. DiMaio, in *Peptides: Structure and Function* (Proceedings of the 8th American Peptide Symposium, 22 to 27 May 1983, Tucson, AZ), V. J. Hruby and D. H. Rich, Eds. (Pierce Chemical Company, Rockford, IL, 1983), p.269.
16. Q. Jiang, A. Seyed-Mozaffari, S. Archer, J. M. Bidlack, *J. Pharmacol. Exp. Ther.* **262**, 526 (1992).
17. R. A. Houghten, *Proc. Natl. Acad. Sci. U.S.A.* **82**, 5131 (1985).
18. J. A. Clark, R. A. Houghten, G. W. Pasternak, *Mol. Pharmacol.* **34**, 308 (1988).
19. L. K. Vaughn *et al.*, *Life Sci.* **52**, 1509 (1993).

20. J. A. Clark *et al.*, *J. Pharmacol. Exp. Ther.* **251**, 461 (1989).
21. R. S. Zukin, M. Eghbali, D. Oliver, E. M. Unterwald, A. Tempel, *Proc. Natl. Acad. Sci. U.S.A.* **85**, 4061 (1988).
22. W. D. M. Paton, *Br. J. Pharmacol.* **12**, 119 (1957).
23. G. Henderson, J. Hughes, H. W. Kosterlitz, *ibid.* **46**, 764 (1972).
24. P. W. Schiller, A. Lipton, D. F. Horrobin, M. Bodanszky, *Biochem. Biophys. Res. Commun.* **85**, 1332 (1978).
25. J. DiMaio, T. M. D. Nguyen, C. Lemieux, P. W. Schiller, *J. Med. Chem.* **25**, 1432 (1982).
26. H. W. Kosterlitz and A. J. Watt, *Br. J. Pharmacol.* **33**, 266 (1968).
27. We thank A. M. Prochera, S. Hope, and P. Lopez for technical assistance, E. Silva for editorial assistance, and NIDA for services provided under contract #271-89-8159. Supported by Houghten Pharmaceuticals Inc. (San Diego, CA) (C.T.D. and R.A.H.); the Medical Research Council of Canada (grant MT-10131 to P.W.S.); and NIDA (grant DA-03742 to J.M.B., grants DA-02615 and DA-000138 to G.W.P., and grant DA-04443 to P.W.S.).

27 June 1994; accepted 25 October 1994

TECHNICAL COMMENTS

A Unified Polymerase Mechanism for Nonhomologous DNA and RNA Polymerases

Extrapolating from the co-crystal structure of rat DNA polymerase β (pol β) complexed with primer-template, dideoxycytidine triphosphate (ddCTP), and two metal ions, H. Pelletier *et al.* (*1*) recently concluded that the orientation of the DNA primer-template in *Escherichia coli* DNA polymerase I Klenow fragment (KF) and the reverse transcriptase (RT) of human immunodeficiency virus–type 1 is opposite to that derived from published co-crystal structures (*2*, *3*). We disagree with this conclusion and suggest an alternative interpretation of the structural data, namely, that there is no contradiction between the orientations of the DNA inferred from these structures; rather, the apparent inconsistency is the result of an inappropriate alignment of the pol β structure with the other polymerase structures. While the crystal structures of KF, RT, and T7 RNA polymerase (RNAP) can be aligned by superposition of a homologous "palm" subdomain, pol β is not homologous to these other polymerases, and therefore should not be aligned with them by superimposing protein structures. Instead, we suggest that pol β can be oriented relative to this family only by superposition of the functionally important entities in the polymerase reaction, namely, the two catalytic divalent metal ions and the 3′ terminus of DNA primer strand. This alignment is achieved by rotating the entire pol β complex by about 180° (Figs. 1 and 2) from the structural alignment proposed by Pelletier *et al.* (*1*). The alignment we suggest allows all four polymerases to use the identical polymerase mechanism on similarly oriented primer-template molecules without the need to re-orient the primer-templates from their previously determined positions and is therefore consistent with structural, biochemical, and molecular genetic studies of polymerase-substrate complexes. [By contrast, the proposal of Pelletier *et al.* (*1*) that the direction of primer-template binding to KF, RT, and RNAP should be reversed contradicts the conclusions drawn from a substantial body of existing data.] A further advantage of our proposed alignment is that it reveals additional analogies between pol β and the other three polymerases in the overall structure of the polymerase domain.

A dominant and consistent feature of all four polymerase structures determined thus far (*4*–*8*) is the existence of a large cleft comprised of three subdomains dubbed "fingers," "palm," and "thumb" by virtue of the anatomical similarity of the polymerase domain to the structure of a right hand (*4*, *5*). The palm subdomain lies at the bottom of the cleft and contains the catalytically essential acidic residues, whose function has been established to be that of binding the metal ions involved in catalysis of the polymerase reaction (*1*, *7*, *9*). The substantial structural similarity in the palm subdomain structures of KF, RT, and RNAP implies that this subdomain is homologous in these three polymerases. By contrast, the corresponding subdomain of pol β is not homologous to those of the three other polymerases, as Davies *et al.* (*7*) and Sawaya *et al.* (*8*) have documented. The palm subdomain of pol β shows some limited structural analogy to the other polymerases in that they all contain a multistranded β sheet with two α helices on one side; however, the topology of the whole pol β palm subdomain is different. Superposition of the Cα positions of the pol β palm subdomain on any of the palm subdomains in the three other structures results in superimposed β strands with opposite orientations. Moreover, the relative positions of the three-metal-ion–binding carboxylates in the ami-

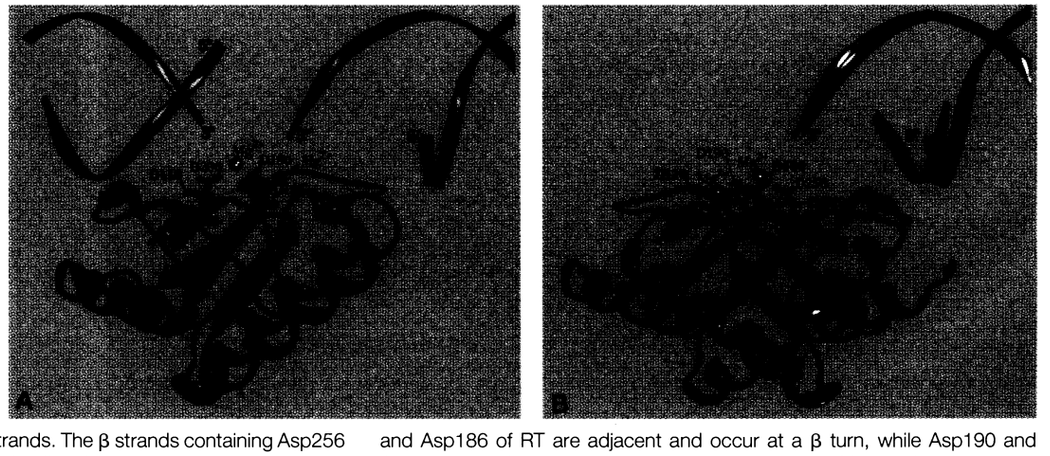

Fig. 1. Alignment of the "palm" subdomains of reverse transcriptase (blue) and pol β (red) and their respective co-crystallized DNAs (*1*, *3*) by (**A**) superimposing the corresponding Cα positions of two α helices and two β strands in the two enzymes, as done by Pelletier *et al.* (*1*), and (**B**) superimposing the 3′ ends of the DNA primer strands in the two complexes. The alignment in (B) was achieved by superimposing the corresponding phosphorous positions at the 3′ end of the DNA primer strands, which puts the metal-binding carboxylates in similar positions, in spite of the lack of superposition of the protein strands. The β strands containing Asp256 in pol β and Asp110 in RT run in opposite directions and are differently ordered relative to the other two carboxylates on the protein sequence. The Asp185 and Asp186 of RT are adjacent and occur at a β turn, while Asp190 and Asp192 of pol β are necessarily separated by one residue so that they occur on the same side of an extended β strand.